A Theoretical Study on the Simultaneous Hydrogen Production and Consumption in Proton Exchange Membrane Fuel Cell/Battery Electric Vehicles

Ahmed Khadhraoui[1], Tarek Selmi[1], Adnen Cherif[1] and Adolfo Iulianelli[2,*]

[1]*ATSSEE Laboratory, Science Faculty of Tunis, university of Tunis Manar, 2092- Tunisia*

[2]*Institute on Membrane Technology of the National Research Council (CNR-ITM), via P. Bucci 17C, Rende (CS), 87036, Italy*

Abstract: Hybrid electric vehicles are new technologies that will be used in future transportation networks in response to the need for sustainable development of environmentally friendly processes. Some of the energy sources used to develop these vehicles are batteries and proton exchange membrane (PEM) fuel cells (FCs), which cannot guarantee the energy required for life in the long term. Electricity storage systems (ESSs) such as the Ultra Batteries (UBs) are suitable candidates for solving the FC transient response issues. The combination of FCs and UBs in electric vehicles is called Fuel Cell Batteries Electric Vehicles (FCBEVs). In this work, an energy consumption model is adopted to simulate the performance of a FCBEV, by considering the power losses of various components, such as the FC, electric motor, the state of charge (SOC) of the battery, and breaks as well as by implementing a reinforcement-learning energy management strategy (EMS), pursuing this scope through the optimization of the hydrogen fuel consumption. In this regard, the motor prototype, after a transient period of around 2.5 min, was able to reach a number of runs equal to 2000, remaining stable for 10 min before coming down to zero.

Keywords: Fuel cell, Fuel cell battery electric vehicle modeling, Energy management, Hydrogen.

1. INTRODUCTION

The ever more pressing requests to pursue a sustainable development, responding to the need of a greener world [1], are involving a relevant attention to an upgrade in transportation technologies. Researchers in both, Academia and Industry, grant significant focus to the transportation system in terms of energy. Up to date, there is no doubt that electric motor driven vehicles, including all EV's types, are the promising solution that has helped to reduce the environmental pollution due to the abatement of greenhouse gases emission in the atmosphere [2]. Electric mobility goals consist of solving the issues related to polluting technologies with a relevant social impact. Electric vehicles (EVs) rely on an electric motor that is sized according to the user [3].

EVs are known to be zero-carbon emission, efficient and do not depend on conventional fuels such as gasoline or petrol. However, still hours are needed to recharge the EV's battery: an issue that has to be addressed. Regarding light of the above, different battery types are still at the laboratory scale or at their early commercial stage, so still the most advanced solution focusses on using the Lithium-ion batteries, thanks to their high-energy storage capacity, low weight, and long lifespan. Battery Electric Vehicles (BEVs) are suffering from the long and balky recharging time. An alternative of BEVs is obviously the Fuel Cell based Electric Vehicles (FCEVs) that need few minutes to refuel the hydrogen tank, as simple as refueling conventional fuels. Furthermore, EVs could use a mixed power system made up of a fuel cell along with back-up battery. Such type of EVs is the so called Fuel Cell Battery Electric Vehicle (FCBEV) [4]. Rezzak and Boudjerda [5] proposed another type of EVs based on a super-capacitor (SC) combined to a FC. Likewise, a hybrid system based on a FC, a battery and a SC has been proposed in [6]. Within this paper, a theoretical study of an enhanced efficiency FCBEV, is presented for the first time During this study, and the simulation results are discussed to highlight and analyze the drive cycle under the so-called "Federal Test Procedure" (FTP-75) of the proposed FCBEV, adopted by the united States to determine the emissions and fuel economy of light-duty vehicles [7]. Accordingly, an Energy Management Strategy (EMS) is implemented to maximize the system's performance through handling the ratio demand/delivery conducted in real-time.

2. METHODS

2.1. The FCBEV Model

The FCBEV presented in Figure **1** uses hybrid electric sources; which are respectively a FC and a battery. A FC is the primary source linked to an unidirectional DC-DC converter to stabilize the output current [8]. A processing system based on water electrolysis is used to produce both, hydrogen and oxygen. A battery, as a second energy source, is connected to a bidirectional DC-DC converter too.

Address correspondence to this article at the Institute on Membrane Technology of the National Research Council (CNR-ITM), via P. Bucci 17C, Rende (CS), 87036, Italy; Tel: +39 0984 492011;
E-mail: a.iulianelli@itm.cnr.it

E-ISSN: 2410-1869/22

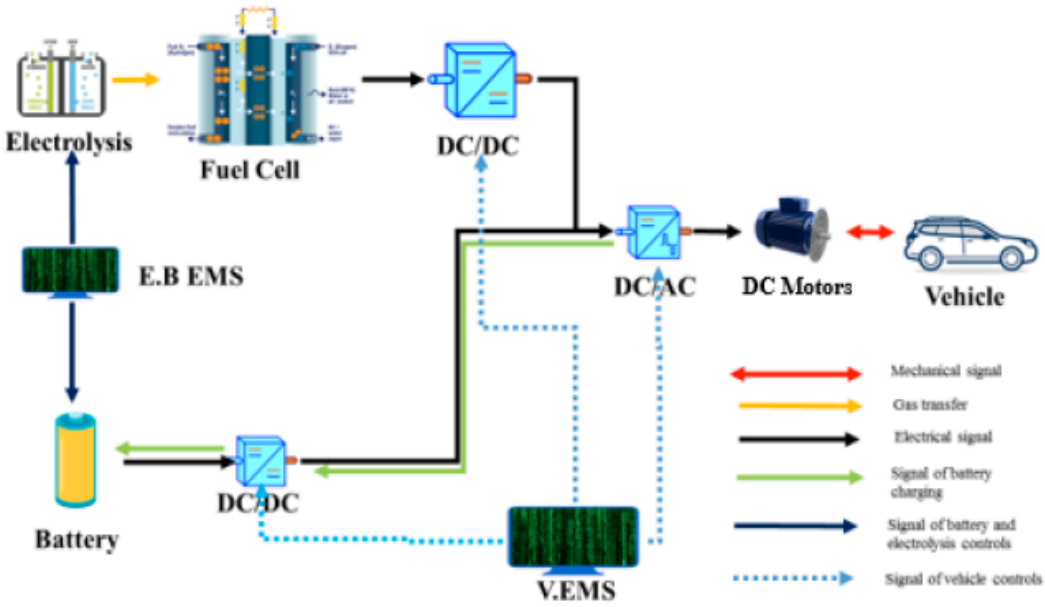

Figure 1: Schematic of the FCBEV structure.

Meanwhile, all the energy sources powers are controlled through an EMS to control the exact amount of hydrogen and at the same time to distribute the power.

2.2. Fuel cell Modeling

Proton exchange membrane fuel cells (PEMFCs) are the most common alternative against batteries within the transport sector and in EV's embedded systems too. The PEMFC consists of: a cathode, an anode, and membrane acting as an electrolyte. The PEMFC is integrated into the electric vehicle system along with auxiliary components such as the electric control unit and the cooling fan to ensure better operations in terms of electricity generation [8,9]. At the anode side, the hydrogen molecules are split into electrons and protons, according to the hydrogen oxidation reaction, presented next, equations (1) and (2):

$$2H_2 \rightarrow 4H^+ + 4e^- \qquad (1)$$

$$2H_2O \rightarrow 4H^+ + 4e^- + O_2 \qquad (2)$$

The hydrogen production of equation (2) is implemented in Matlab/Simulink as shown in Figure **2**.

Table **1** presents the electrolyser parameters used in the model.

While Figure **3** shows the electrical model of a battery; the vacuum voltage (E_{nernst}) is dropped through the activation (V_{act}), the ohmic resistance (V_{ohm}), and the concentration (V_{com}), respectively. The FC voltage is calculated by subtracting the losses from the open-circuit voltage of the FC. The potential of the FC, at any time, could be found using equation (3) based on the parameters of Table **2**.

$$\begin{cases} V_{stack} = N_{cell}.V_{cell} \\ V_{stack} = N_{cell}.(E_{nernst} - V_{act} - V_{ohm} - V_{com}) \end{cases} \qquad (3)$$

Where the energy (E) is expressed as:

$$E = E^0 + \frac{RT}{F} Ln\left(\frac{PH_2PO_2^{0.5}}{PH_2O}\right) \qquad (4)$$

Table 1: Input Parameters for PEM Electrolysis Modeling [10]

Parameters	Values
Partial pressure of oxygen P_{O_2}(atm)	1.0
Partial pressure of hydrogen P_{H_2}(atm)	1.0
Activation energy at the anode $E_{A,a}$ (KJ/mol)	76
Activation energy at the cathode $E_{A,c}$, (KJ/mol)	18
Water contents at the anode-membrane, λ_a	14
Water contents at the cathode-membrane , λ_c	20

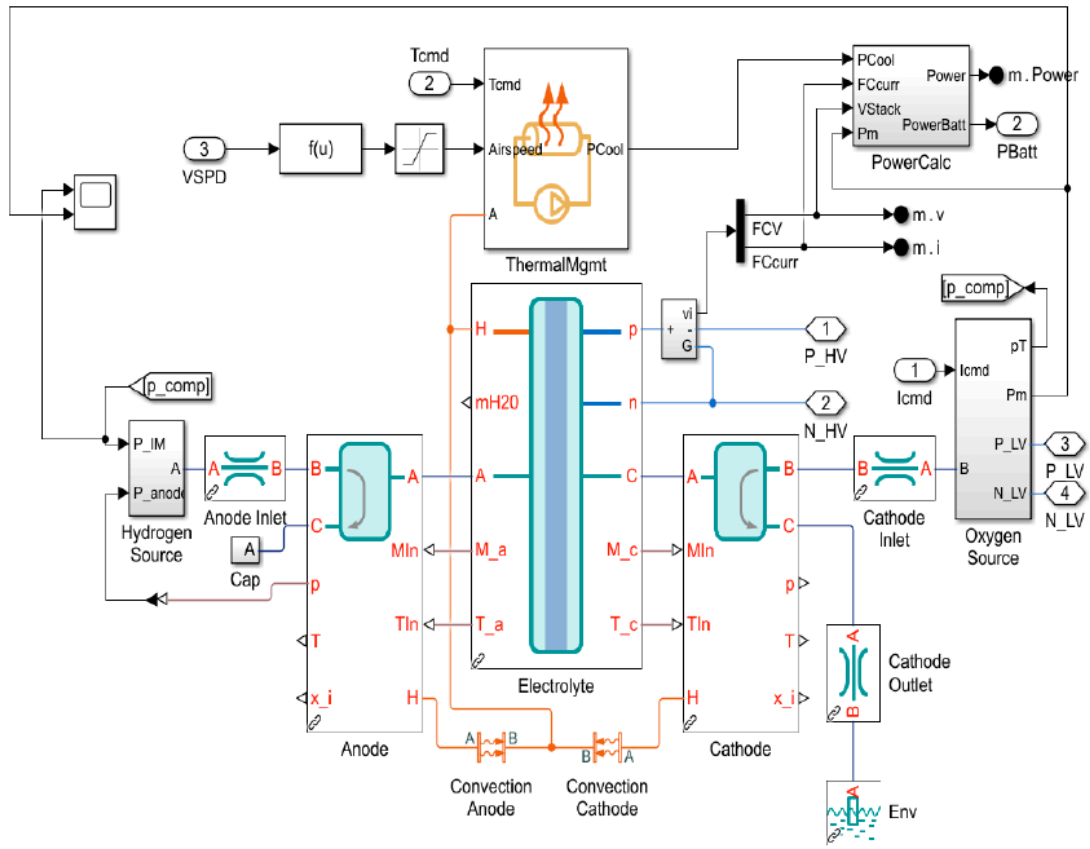

Figure 2: Schematic of the water electrolyser by Simulink.

However, the activation voltage depends on the kinetic phenomena and the oxygen concentration as presented in equation (5) through (7).

$$\begin{cases} V_{act} = [\xi_1 + \xi_2.T + \xi_3.T.Ln(C_{O_2}) + \xi_4.T.Ln(I)] \\ C_{O_2} = \frac{P_{O_2}}{5.08*10^6 e^{-498/T}} \end{cases} \quad (5)$$

$$\begin{cases} V_{ohm} = R_m.I & (6) \\ R_m = \rho_m.l/A & (7) \end{cases}$$

$$E_{Nernst} = 1.229 - 0.85 * 10^{-3}(T - 298.15) + 4.3085 * 10^{-5}T\left[\ln(P_{H_2}) + 0.5 * ln(P_{O_2})\right] \quad (8)$$

$$V_{com} = -B\left(1 - \left(I/J_{max}\right)\right) \quad (9)$$

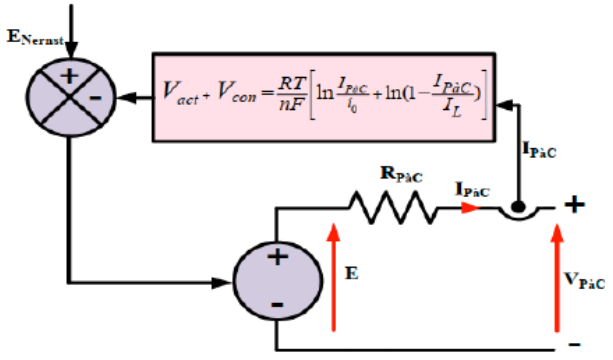

Figure 3: Equivalent Electrical model of a PEM Fuel Cell.

Table 2: PEM fuel Cell Parameters

Parameter	Value
Fuel cell area	280 cm^2
Membrane typology	Nafion115
Membrane thickness	125 µm
Exchange current density	exp(-5.4) A/cm^2
Max current density	1.4 A/cm^2
Transfer coefficient	0.5
Membrane dry density	$2x10^{-3}$ kg/cm^3
Membrane dry weight	1.1 kg/mol

2.3. Battery Modeling

The complex electrochemical phenomena involved in a battery make its modeling tricky. Detailed models exist and take into account, for example, the concentration of reagents or the influence of temperature. These very detailed models are difficult to be adopted in the energy context of interest. Other types of models based on equivalent electrical diagrams (ideal voltage generators, resistors, capacitors, etc.) provide accurate account of the battery's electrical behavior [11], according to the parameters illustrated in Table **3**. The equivalent electrical model of the battery retained during this work is illustrated in Figure **4**. The diagram consists of a voltage generator and a resistance in series. The

elements in this diagram (V_{oc} vacuum voltage and R_{int} load and discharge internal resistance) depend on the state of charge (SOC) of the battery.

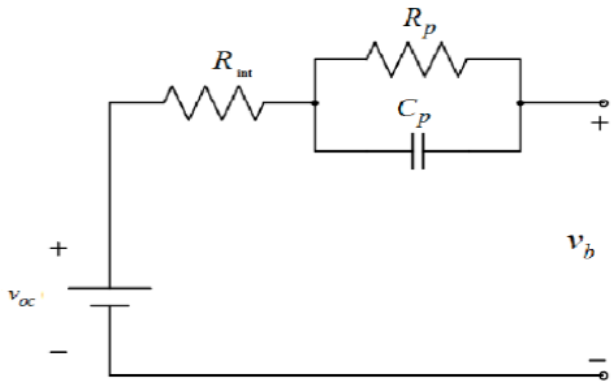

Figure 4: Equivalent Battery model.

The current of the battery may be calculated as in equation (10):

$$I = V_{oc} - \sqrt{\frac{V_{oc}^2 - 4R_{int}P_{actual}}{2R_{int}}} \qquad (10)$$

$$V_{term} = V_{oc} - IR_{int} \qquad (11)$$

The new state of charge "SOC_{new}" is given by the equation centered on the old "SOC_{old}", equation (12)

$$SOC_{new} = SOC_{old} + 100\left(\frac{dE_{int}}{E}\right) \qquad (12)$$

The ideal power "P_{ideal}" may be calculated following equation (13):

$$P_{ideal} = P_{actual} + P_{loss} \qquad (13)$$

where

$$P_{loss} = I^2R_{int} \qquad (14)$$

$$P_{ideal} = IV_{OC} \qquad (15)$$

$$P_{actual} = IV_{OC} - I^2R_{int} \qquad (16)$$

Table 3: Battery Parameters

Parameter	Value
Pack Voltage	272.9 V
Capacity	3.2 Ah
SOC	60%
Temperature	27 C
$SOC\ Bat\ max$	90%
$SOC\ Bat\ min$	20%

2.4. Vehicle Modeling

This amount of energy needed to run a vehicle (E_v) can be calculated through the dynamic behavior of the car, equation (17) [12], described by the classic equations of mechanics, depending on the power (P_v) provided at the level of the wheels, whereas the related parameters are presented in Table **4**.

$$E_v = \int_0^t P_v\, dt \qquad (17)$$

P_v is expressed as a function of the total traction torque, C_T, and the wheel speed, Ω_r, as follows:

$$P_v = C_T\, \Omega_r \qquad (18)$$

$$C_T = F_{tr}.r\ ;\ \Omega_r = \frac{v}{r} \qquad (19)$$

F_{tr} represents the tractive force acting on the vehicle at the contact level between the tires of the driving wheels and the road surface, enabling the vehicle to be propelled forward, v and r, the vehicle's-imposed speed and wheel radius, respectively.

Thus, according to Newton's second law, the acceleration needed to overcome the inertia of the vehicle and thus to allow the acceleration of the vehicle, α, can be expressed by equation (20):

$$\alpha = \frac{F_{tr} - (F_{aero} + F_{grade} + F_{rr})}{m_i} \qquad (20)$$

The F_{tr} value needed to overcome the resistance to advance and accelerate the vehicle may be calculated by equation (21):

$$F_{tr} = F_{aero} + F_i + F_{grade} + F_{rr} \qquad (21)$$

F_{aero} is the aerodynamic force, representing the resistance of air depending on the direction of the vehicle movement. It depends on the air density, the frontal surface A_F, the air penetration coefficient, C_d, of the vehicle and the vehicle speed, V. It is represented by equation (22):

$$F_{aero} = \frac{1}{2}\rho C_d A_f V^2 \qquad (22)$$

F_{rr} is the rolling force, which represents the rolling resistance of the vehicle, acting at the level of the contact between the tyres and the roadway and is opposed to the free movement of the vehicle. This force must be contrasted to push a vehicle out of fuel at a constant speed. It is proportional to the mass of the vehicle, M, the gravitational acceleration, *g*, and the rolling resistance coefficient, C_r as shown in equation (23)

$$F_{rr} = mgC_{rr} \qquad (23)$$

F_{grade} is the gravity force of the vehicle, acting directly on the vehicle on the slopes. It holds it uphill

and pushes it downhill. This force is a function of the slope inclination as well as the vehicle mass. The expression of this force is given by equation (24):

$$F_{grade} = mg\sin(\theta) \qquad (24)$$

The sum of the above-mentioned forces leads to the traction force, which is schematically illustrated in Figure **5**.

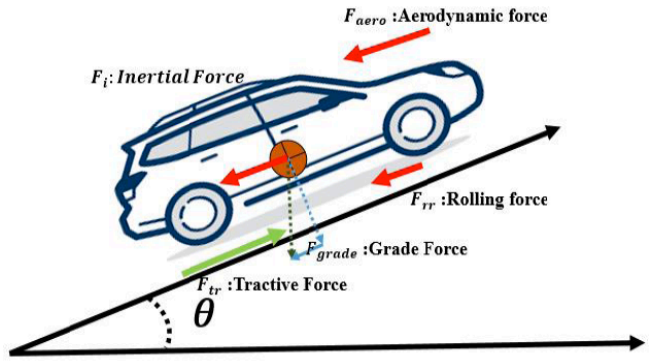

Figure 5: Schematic of the tractive forces acting on a vehicle.

Table 4: Vehicle Parameters

Parameter	Value
Vehicle's mass	1300 K_g
Gravity	9.8 m/s^2
Air density	1.18 kg/m^3
Road angle	0.5 °

2.5. Energy Management System

The energy management system (EMS) plays an important and significant role in the ratio stored/needed energy. Besides, it helps to harvest extra power during breaking phases, especially within the city.

2.5.1. Type of Energy Management Systems

There are three principal methods of energy optimization:

- The dynamic programming method; this EMS is not particularly used due to its low efficiency [13]

- The Optimal control method; it shows higher performance and operates on real-time [14]

- The Intelligent technique; it is a neural network-based model, needing fast digital signal processors (DSP) [15].

2.5.2. Energy Management System Proposed

Two algorithms make the proposed EMS within this paper. One is used for the electrolysis by the battery current and is called electrolysis battery EMS (E.B.EMS). The second algorithm controls all the parts of the vehicle model and is called Vehicle EMS (V.EMS).

2.5.2.1. E.B.EMS

The E.B.EMS receives two input parameters, namely SOC and Vehicle Power ($P_{vehicle}$). The E.B.EMS response in terms of desired amount of hydrogen produced depends on the input parameters, Figure **6**.

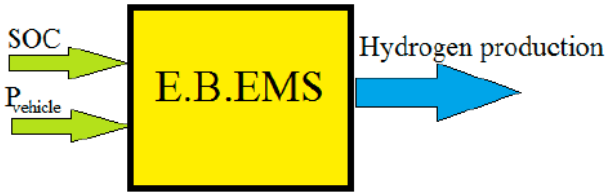

Figure 6: Global structure of the electrolysis battery energy management strategy (E.B.EMS) for hydrogen production by battery assisted water electrolysis.

The operating modes, shown in Figure **7**, denote the possible position of a vehicle, namely the "stop" and "hydrogen production" modes, respectively.

2.5.2.2. V.EMS

The V.EMS is based on five parameters, which are provided as inputs to obtain the desired level of FC power at the output side, Figure **8**. The power to be

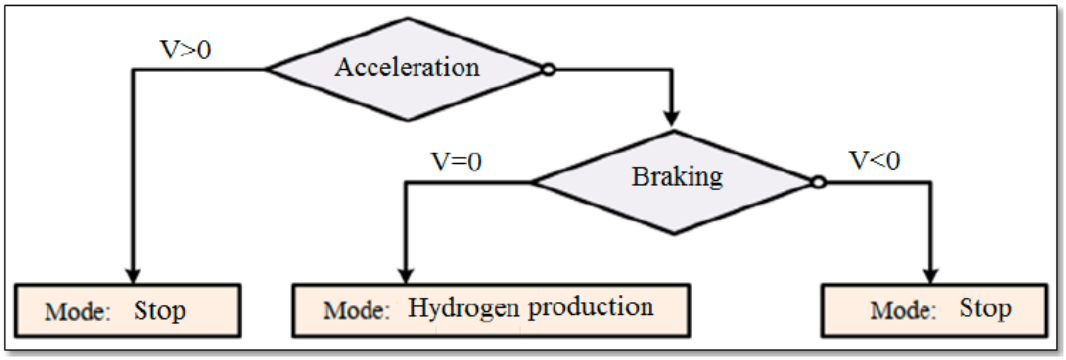

Figure 7: Schematic of the vehicle operating modes.

supplied by the FC is determined on the cornerstone of the power demanded by the vehicle as well as the variation of the state of charge of the battery indicated as SOC_{Bat}.

Figure 8: Global structure of the algorithm used for the Vehicle Energy Management Strategy (V.EMS).

The control has to monitor in real-time the SOC_{Bat} in order to be ready to respond in all times to the vehicle's power demands, while avoiding full charge as well as deep discharge. The equation (25) describes the power transfer between the FC, the battery, and the charge.

$$P_{Ch} = P_{FC} + P_{Bat} \qquad (25)$$

It is a common practice that the deep discharge and overload situations could dramatically damage any type of battery. Accordingly, equation (25) has been taken into consideration within the proposed model to avoid both situations for the sake of better reliability. This is to say, the battery voltage is strictly between V_{Bat_min} and V_{Bat_max} as expressed in equation (26).

$$V_{Bat\_min} < V_{Bat} < V_{Bat\_max} \qquad (26)$$

3. RESULTS AND DISCUSSION

The EMS role is to control the system's components. The algorithm of the EMS shown in Figure **9** has been implemented in Matlab Simulink in order to highlight its efficiency and reliability.

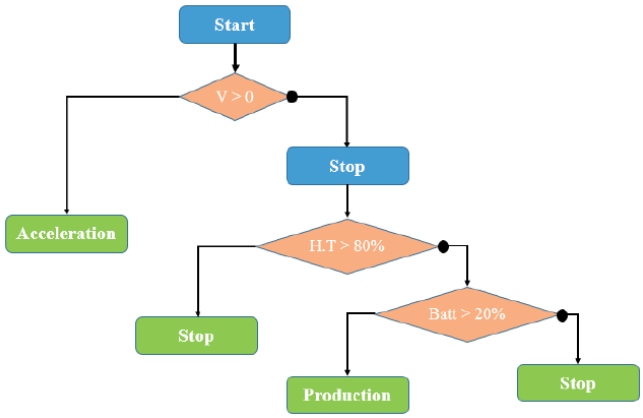

Figure 9: Schematic of the Enery Management Strategy (EMS) algorithm structure proposed.

The model was tested under the European driving cycle ECE-15 for 200 seconds (it is one of the cycles used to measure the performance degree of the vehicles engines and energy economy in passengers [12, 16]). The results obtained from the simulation focused on the evaluation of the sources. The obtained results of the vehicle speed are in full agreement with the expected ones, as shown in Figure **10**.

To describe as close as possible a vehicle under real operation, many "stop mode" in the cycle were considered as reported in the latter figure, such as: 0 - 15s, 25 - 50s, 95 - 115s, 190 - 200s. This approach involved a clear vision for the current and the hydrogen production in the model. However, the battery response is faster than the FC, as clearly shown in Figure **11**.

In order to model the generation of hydrogen by water electrolysis, the simulation of the vehicle standing on "stop mode" is based on the electricity utilization to develop the electrolysis process obtained from the battery. When they are part of the stop in the drive cycle, the EMS tests the hydrogen tank and, in case its volume is less than 80%, the FC will create

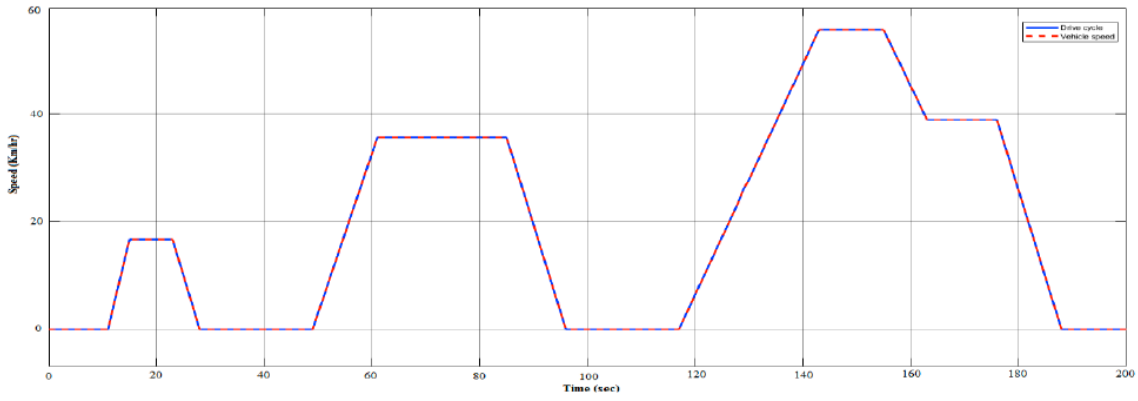

Figure 10: Simulation results on the vehicle speed (km/hr) vs time (sec) according the European driving cycle ECE-15 tests for measuring the performance degree of the vehicles; range time adopted during the simulations: 200 sec.

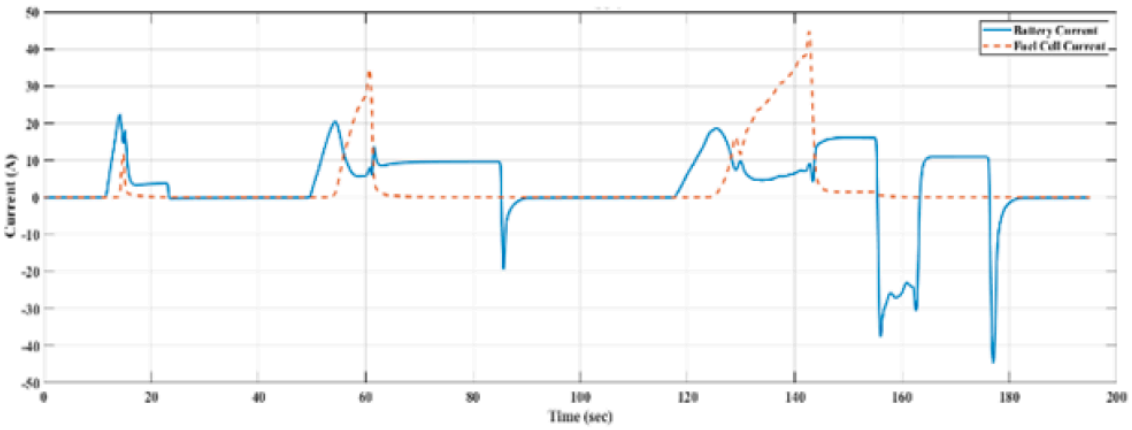

Figure 11: Battery and FC current responses vs time.

more hydrogen. This is to say, when the vehicle is not running (Stop mode) and the hydrogen quantity in the vehicle's tank is less than 80%, the FC becomes supplied from the battery to produce hydrogen and fill the missing amount. This approach has been implemented in the Simulink model of the EMS and the results are shown in Figure **12**.

The ECE-15 is not known to be the most suitable in terms of profitability tests. Therefore, the drive cycle was changed to the FTP-75 with 1400 seconds in duration. The EMS is simulated through the vehicle speed variation, represented in Figure **13**, which allowed to obtain the simulation results shown in Figure **15**, representing the FC and battery current as a function of operation time.

Between almost 18 km driving distance and 34.1 km/h average speed, Figure **13** shows three phases of cruise. Between 0s and 505s, which consists of a cold

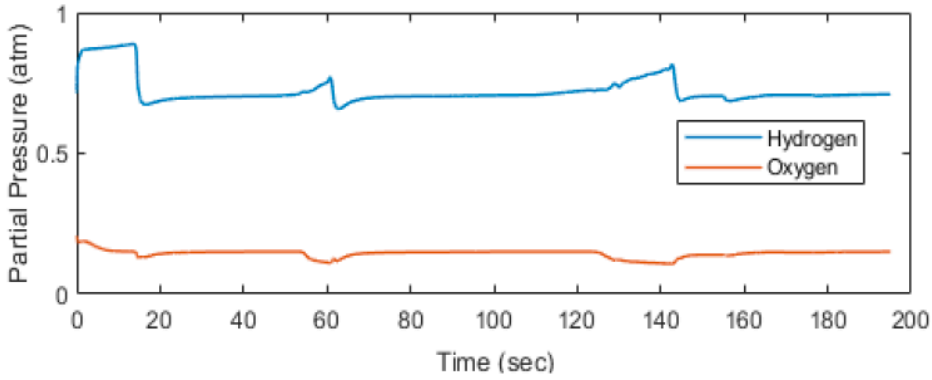

Figure 12: Production of hydrogen by water electrolysis vs time (sec), during the simulation of the vehicle standing on "stop mode". The electrolysis process is developed using the electricity coming from the battery

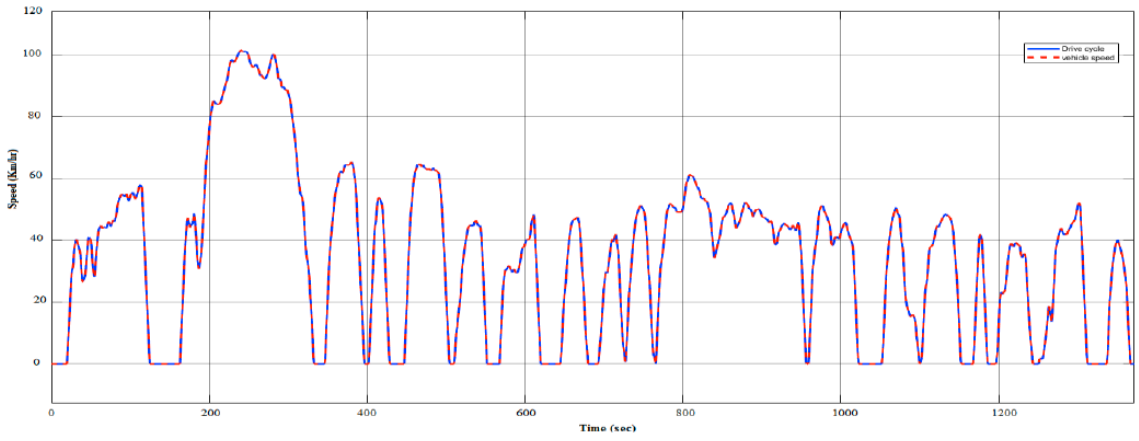

Figure 13: The Energy Management Strategy is simulated through the vehicle speed variation (km/hr) vs time (sec).

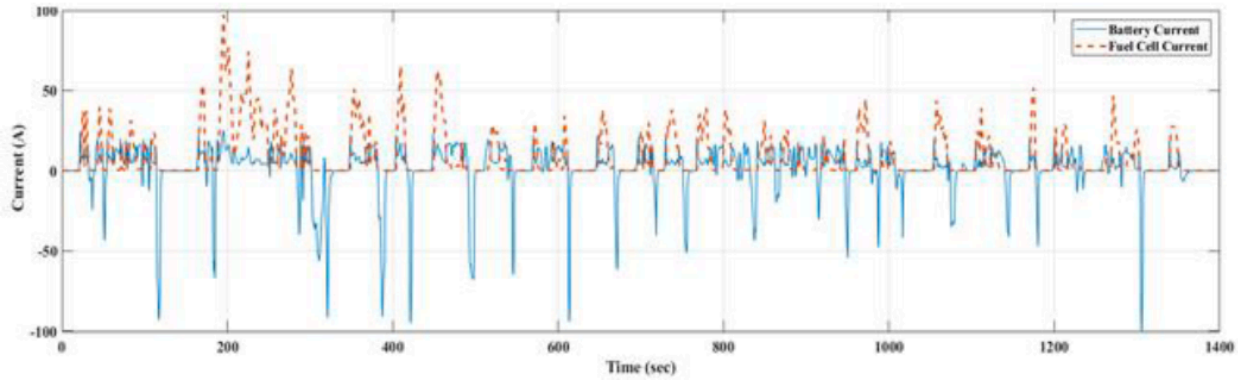

Figure 14: Power supply due to the FC and Battery currents (A) vs time (sec).

start transient phase, many variations between the intermediate and the high speed are recorded. Then, between 506s and 1372s, the speed becomes more stable at an intermediate value and the restant speed cycle is a stop mode.

Figure **14** illustrates the current of the two sources according to the adopted strategy. The response of the FC is slow; indeed, the battery takes the action since the FC does not provide power when sudden demand happens. Thus in Figure **14**, the battery's voltage decreases or increases according to the sign of the current given by the speed profile of Figure **13**, in which the SOC decreases from 60% to 48.5%, Figure **15**. In the figure, some recharging periods are considered in the time ranges [303s, 310s], [490s, 503s] etc.

According to the simulation results, the proposed energy management system (EMS) is efficiently handling the following tasks:

1. Check the drive cycle
2. During the acceleration phase, energy is being absorbed from both sources, FC and battery
3. During the breaking phase, the FC is not providing energy anymore; at the same time, the battery is charging
4. Within the urban zone, when high acceleration is not needed, the energy is totally provided by the FC.

Such results are clearly shown in Figures **11** and **14**. In fact, when the vehicle is running, the FC provides almost 85% of the needed current, while the battery is providing rest. When the FC's current (Red dashed curve) is at zero, the battery's current (Blue solid line) is negative which means that the battery is receiving current (Positive when it is delivering current).

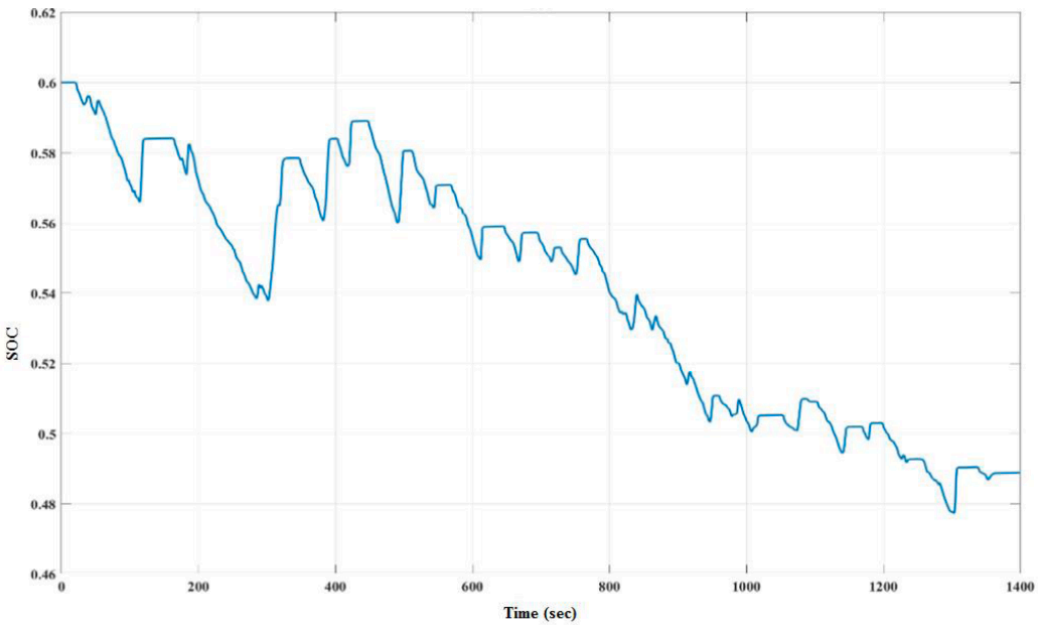

Figure 15: State of Charge (SOC) of the Battery (ranging between 0 and 1) vs time (sec).

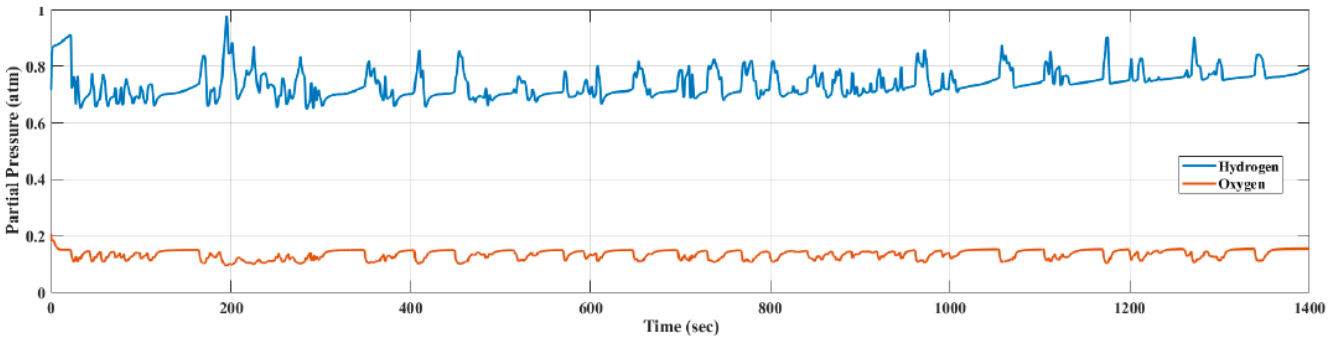

Figure 16: Production of hydrogen and oxygen vs time during the vehicle standing under “stop mode”.

Figure **15** shows that the initial charge of the battery was at 60%, at the end of the cycle, the battery becomes at almost 49%. This means that 11.04 miles (17.77 km), the battery has discharged by 11%.

According to the results sketched in Figures **13**, **14**, the FC ensures the required energy as a primary source because of the hydrogen consumption. Hence, the vehicle does not consume much power from the battery according to the SOC. Indeed, the vehicle produces hydrogen each time when a stop mode is considered, contributing to the economy of the whole system, Figure **16**.

In order to validate the EMS proposed, the FCBEV mode was simulated and experimentally validated for a fuel cell-based vehicle using a DC motor for a lab scale prototype.

Table 5: Parameters used for the Fuel Cell Prototype

Element	Parameter	Value
Fuel cell	Operating voltage	0.9 V
	Operating current	600 mA
	Rated power	300 mW
	Hydrogen storage capacity	20 mL

Figure 17: Fuel cell prototype.

According to the parameters of Table **5**, which are those of the real FC of Figure **17**, the FC prototype was first simulated in order to generate hydrogen for a tank of 20 ml, Figure **18**. As shown in the latter figure, the target hydrogen volume was produced at steady state condition after around 120s.

After the production of hydrogen and according to the parameters of Table **6**, Figure **19** illustrates the motor prototype performance in terms of number of runs against the time. After a transient period of around 2.5 min, several runs equal to 2000 were reached,

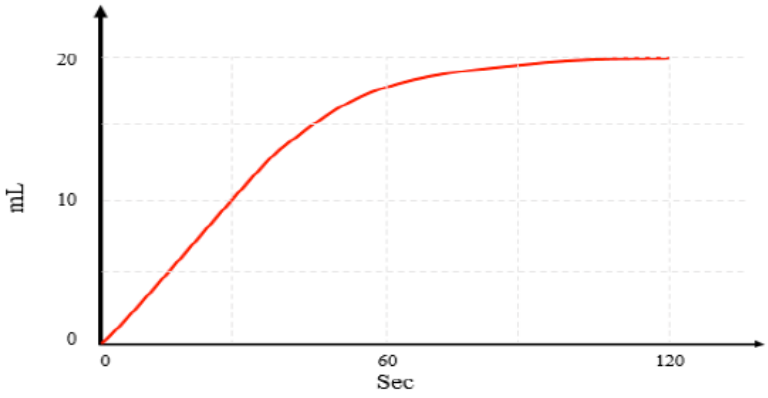

Figure 18: Volume of produced hydrogen vs time.

which remained stable for 10 min before coming down to zero.

Table 6: Parameters of the Motor Prototype

Element	Parameter	Value
Motor	Voltage	1 - 3 V
	current	1 A
	Tour number	2000 Tr/min
Battery	Voltage	3.7 V
	current	2.5 A

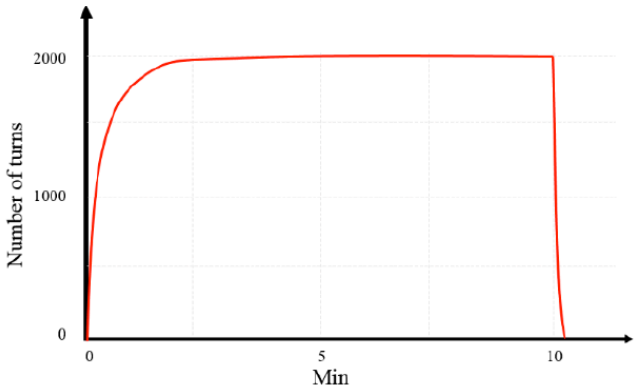

Figure 19: Motor function in terms of number of runs as a function of time.

5. CONCLUSIONS

This paper presented the energy management systems fuel cell/battery electric vehicles. In particular, the fuel cell/battery electric vehicles modeling was first resumed, and then a monitoring and management system was developed and analyzed in details by highlighting the structure and performances. The analysis of the fuel cell/battery electric vehicles focused on hydrogen consumption and the need of recharging the battery for maximizing the 'charge sustaining' and cost reduction. The electrolysis battery energy management system played a relevant role in the production of hydrogen as the main source of the fuel cell when the vehicle stops, contributing to the performance enhancement of the electric vehicle. The latter aspect could contribute also to better design the new electric vehicles, declassing the importance related to the presence of hydrogen filling stations, not yet available everywhere.

The simulations presented in this work were validated by adopting the energy management system, which allowed to operate an electric motor prototype efficiently and robustly under rapid changes in power demand, and different levels of the state of charge. The model was tested under the European driving cycle ECE-15, representing one of the reference cycles used to measure the performance degree of the vehicles engines and energy economy in passengers, and the obtained results of the vehicle speed resulted in full agreement with the reference ones. In particular, the motor prototype, after a transient period of around 2.5 min, was able to reach a number of runs equal to 2000, remaining stable for 10 min before coming down to zero. Last but not least, this study demonstrated that, once the vehicle was running, the FC may provide almost 85% of the necessary current, whereas the rest may be provided by the battery, which initially showed a status of charge equal to 60% and, at the end of the cycle, was decreased to 49%.

In a future work, the theoretical analysis of the performance of an electric vehicle realized by adopting an energy management system will be substituted by the fuzzy logic approach, implementing experiments to validate a fuel cell/battery electric vehicle combined with solar power.

REFERENCES

[1] Committee, Climate Change. The UK's contribution to stopping global warming. 29 May 2019. https://www.theccc.org.uk/publication/net-zero-the-uks-contribution-to-stopping-global-warming/ (accessed October 2, 2022).

[2] Ingeborgrud L, Ryghaug M. The role of practical, cognitive and symbolic factors in the successful implementation of battery electric vehicles in Norway, Transportation Research Part A: Policy and Practice, 2019; 130: 507-516. https://doi.org/10.1016/j.tra.2019.09.045

[3] Andwari MA, Apostolos P, Srithar R, Martinez-Botas R, Vahid E. A review of Battery Electric Vehicle technology and readiness levels, Renewable and Sustainable Energy Reviews, 2017; 78: 414-430. https://doi.org/10.1016/j.rser.2017.03.138

[4] Lü X, Xing M, Wenming L, Lü J. Extension control strategy of a single converter for hybrid PEMFC/battery power source, Applied Thermal Engineering, 2018; 128: 887-897. https://doi.org/10.1016/j.applthermaleng.2017.09.003

[5] Rezzak D, Boudjerda N. Management and control strategy of a hybrid energy source fuel cell/supercapacitor in electric vehicles, International Transactions on Electrical Energy Systems, 2017; 27: e2308. https://doi.org/10.1002/etep.2308

[6] Zhan Y, Guo Y, Zhu J, Li L. Power and energy management of grid/PEMFC/battery/supercapacitor hybrid power sources for UPS applications, International Journal of Electrical Power & Energy Systems, 2015; 67: 598-612. https://doi.org/10.1016/j.ijepes.2014.12.044

[7] Zhao X, Zhao X, Qiang Y, Yiming Y, Man Y. Development of a representative urban driving cycle construction methodology for electric vehicles: A case study in Xi'an, Transportation Research Part D: Transport and Environment, 2020; 81: 102279. https://doi.org/10.1016/j.trd.2020.102279

[8] Alaswad A, Omran A, Sodre JR, Wilberforce T, Pignatelli G, Dassisti M, Baroutaji A, Olabi AG. Technical and Commercial Challenges of Proton-Exchange Membrane (PEM) Fuel Cells. Energies, 2021; 14: 144. https://doi.org/10.3390/en14010144

[9] Paturzo L, Basile A, Iulianelli A, Jansen JC, Gatto I, Passalacqua E. High temperature proton exchange membrane fuel cell using a sulfonated membrane obtained via H2SO4 treatment of PEEK-WC, Catalysis Today, 2005; 104: 213-218. https://doi.org/10.1016/j.cattod.2005.03.050

[10] Ni M, Leung MKH, Leung DYC. Electrochemistry Modeling of Proton Exchange Membrane (PEM) Water Electrolysis for Hydrogen Production, 16th Word Hydrogen Energy Conference, 13-16 June 2006 – Lyon France, pp. 1-7.

[11] Li X, Wang Y, Yang D, Chen Z. Adaptive energy management strategy for fuel cell/battery hybrid vehicles using Pontryagin's Minimal Principle, Journal of Power Sources, 2019; 440: 227105 https://doi.org/10.1016/j.jpowsour.2019.227105

[12] Khadhraoui A, Selmi T, & Cherif A. Energy Management of a Hybrid Electric Vehicle. Engineering, Technology & Applied Science Research, 2022; 12(4): 8916-8921. https://doi.org/10.48084/etasr.5058

[13] Wahib A, Ghozzi S, Hatem A, Mami A. Design, modeling and energy management of a PEM fuel cell/supercapacitor hybrid vehicle, Int J Advanced Computer Sci Appl, 2017; 8: 1. https://doi.org/10.14569/IJACSA.2017.080135

[14] Truong HVA, Dao HV, Do TC, Ho CM, To XD, Dang TD, Ahn KK. Mapping Fuzzy energy management strategy for PEM fuel cell–battery–supercapacitor hybrid excavator, Energies, 2020; 13: 3387. https://doi.org/10.3390/en13133387

[15] Abdolrasol MGM, Hussain SMS, Ustun TS, Sarker MR, Hannan MA, Mohamed R, Ali JA, Mekhilef S, Milad A. Artificial Neural Networks based optimization techniques: a review. Electronics, 2021; 10: 2689. https://doi.org/10.3390/electronics10212689

[16] Li S, Jin Y, You F. Sustainable residential micro-cogeneration system based on a fuel cell using dynamic programming-based economic day-ahead scheduling, ACS Sustain Chem Eng, 2021; 9: 3258-3266. https://doi.org/10.1021/acssuschemeng.0c08725

Received on 15-09-2022 Accepted on 13-10-2022 Published on 18-10-2022

DOI: https://doi.org/10.15379/2410-1869.2022.09